SAND2022-12140C

Efficient WEC Array Buoy Placement Optimization with Multi-Resonance Control of the Electrical Power Take-off for Improved Performance

Madelyn G. Veurink[1], Wayne W. Weaver[1], Rush D. Robinett III[1], David G. Wilson[2], Ronald C. Matthews[2]
[1]Michigan Technological University, Houghton, MI 49931, USA,
[2]Sandia National Labs, Albuquerque, New Mexico 87123, USA

***Abstract*—An array of Wave Energy Converters (WEC) is required to supply a significant power level to the grid. However, the control and optimization of such an array is still an open research question. This paper analyzes two aspects that have a significant impact on the power production. First the spacing of the buoys in a WEC array will be analyzed to determine the optimal shift between the buoys in an array. Then the wave force interacting with the buoys will be angled to create additional sequencing between the electrical signals. A cost function is proposed to minimize the power variation and energy storage while maximizing the delivered energy to the onshore point of common coupling to the electrical grid.**

***Index Terms*—Wave energy converters, Energy capture, Multi-resonance control, Renewable energy, Power packet Networks**

I. Introduction

In order for WECs to be implemented on all coast lines the energy capture of these renewable energy sources (RESs) must be maximized while the operating costs, component sizing and power losses must be minimized. To economically capture the large amount of energy in the ocean's surrounding the United States the energy conversion from wave-to-wire needs to be maximized [1], [2]. RESs currently need Energy Storage Systems (ESS) and additional power electronics to provide suitable power to the grid. The ESS, although necessary for producing a stable power output, has a large installation cost that can impact the levelized cost of energy (LCOE). Minimizing the size of the ESS and utilizing new advances in power electronics, and power packet networks (PPN), the wave-to-wire efficiency of WECs will increase and create a more robust and stable coupling to the grid [3].

To create electricity from the ocean's waves a power-take-off (PTO) on the buoy of the WEC can be utilized to transform the vertical heaving motion of the buoy into a rotational velocity. The rotational velocity of the rack-and-pinion PTO can be coupled to an electric machine on the buoy which will generate electricity [4]. The ac power is converted to dc before being stored in a dc bus where it is then transported to shore at a constant voltage via an undersea cable before coupling to the grid [5]. To maximize the power generation of an individual buoy the buoy must resonate with the dominant frequencies of the wave it is operating in.

The wave environment that a WEC operates in can be modelled by an irregular sine wave composed of many different frequency components. The irregular wave environment can be described with a Bretschneider Spectrum which is generated using the significant wave height and peak frequency of the sea state [6]. The Bretschneider spectrum is used to to describe the sea-state in a location at a certain time.

To maximize the energy production of a WEC in any given sea-state it must be able to resonate with the dominate frequencies of the wave force [7], [8], [1]. Complex Conjugate Control (C3) requires that the WEC resonates with the excitation force and that the added damping of the controller is equal in magnitude to the damping of the WEC system [9], [10].

To implement C3 in the time domain the magnitudes and phases of the wave spectrum's frequency components need to be calculated [7], [8], [1]. The magnitudes and phases of the time domain frequency components are then used within a proportional derivative (PD) feedback loop where the proportional gain is calculated using the magnitudes of the decomposed frequencies and the derivative gain is set equal to the mechanical impedance [7], [8], [1], [11]. The time domain implementation of C3, Proportional Derivative Complex Conjugate Control (PDC3) was implemented in [12]. C3 was implement on a nonlinear WEC to maximize energy capture and limit the size of the ESS by altering the buoy to generate the necessary reactive power through its unique shape [13].

Multiple WECs with PDC3 control can be arranged in a configuration that will improve the wave-to-wire efficiency of the system and increase the delivered grid power of the array by using PPN technologies [14]. Early PPN technology was explored in [15] as Electricity Power Packets (EPP) as a way to incorporate RESs into an Open Electric Energy Network. By using PPNs to minimize the size and losses of the ESS in a WEC array the power delivered to the grid can be maximized.

This work will utilize the work done in [12] and [14] to develop a hexagonal array of six wave energy converters to create a PPN. The physical location of the WECs in the array will be shifted to create an advantageous phasing in the electrical signals to produce minimal losses in the ESS and maximize the wave-to-wire efficiency of the system. In addition to shifting the spacing of the buoys in relation to each other the angle of the incident wave force interacting with the buoys will be adjusted to further minimize the losses due to noise in the ESS and reduce the effect the oscillatory nature of the waves has on the power delivered to the grid. In addition

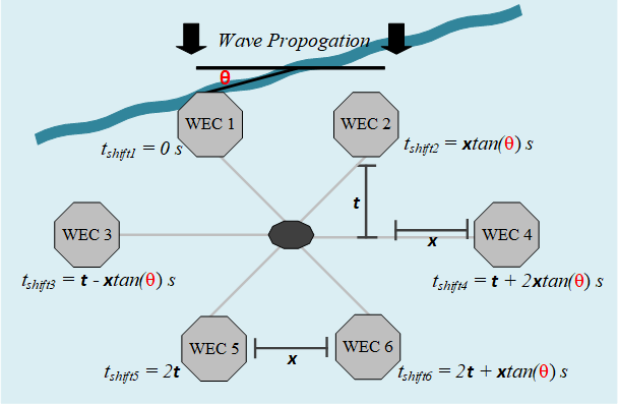

Fig. 1. Hexagonal Arrangement of the Six WEC Array.

to the spacing between the WECs and the angling of the incident wave force, the grid update rate will also be utilized to minimize a cost function. The cost function is designed to maximize the energy delivered to the grid while minimizing the power variation in the WEC array.

II. Electrical and Mechanical Model of WEC

The main components of a WEC include a buoy, an electric machine, an ESS, a line to shore, and the electric grid integration. Multiple WECs with electric machines can be connected to the same ESS, in parallel, to create a WEC array. The positioning of the buoys in a 6 WEC array is shown in Figure 1 where pairs of WECs are shifted spatially in the water to create phasing in their electrical signals with respect to each other.

The mechanical system of the WECs absorbs the power from the wave by converting it from heaving motion into a rotational velocity. The rotational velocity turns an electric machine on each of the six WECs in the array where the power is then sent to an undersea substation. [4] provided the basis for the mechanical and electrical modelling in this study.

A. Mechanical Drive-Train

Each of the buoys' mechanical systems in the WEC array can be modelled as a mass-spring-damper differential equation

$$m\ddot{x_i} + c_i\dot{x_i} + kx_i = f_{e,i} + f_{u,i}. \tag{1}$$

The excitation force on each of the WECs in the array, $f_{e,i}$, is phase shifted due to the physical placement of the buoys in the water. The control force, $f_{u,i}$, has the same phase shift as the excitation force. The controller is actuated on each of the WECs through the linear force of the permanent magnet DC machine as

$$f_{u,i} = \frac{\tau}{r} = \frac{i_{a,i}K_m}{r} \tag{2}$$

where K_m is the permanent magnet DC machine torque constant and r is the radius of the rack-and-pinion gear.

The rotational velocity used to turn the electric machines on each of the buoys is generated through the rack-and-pinion PTO. The PTO converts the heaving linear motion of the buoy into a rotational velocity through the gear radius as

$$v_i = \dot{x_i} = rw_{m,i} \tag{3}$$

where v_i is the linear velocity of the buoy, r is the gear radius, and $w_{m,i}$ is the rotational velocity of each of the electric machines. The rack-and-pinion gear system is used to turn the electric machine on each of the buoys and generate power.

B. Electrical Drive-Train

The electrical system on each of the buoys is made of: an electric machine, a DC bus, a line to shore and the grid tie inverter. The electrical system on each of the buoys can be modelled as

$$\dot{i_{a,i}} = \frac{1}{L_a}(v_{a,i} - i_{a,i}R_a - \frac{K_m v_i}{r}). \tag{4}$$

The power that is produced by each of these electric machines is sent to the electrical bus as

$$i_{pto,i} = \frac{P_{pto,i}}{v_b} = \frac{v_{a,i}i_{a,i}}{v_b}. \tag{5}$$

The electric machines on the six buoys are connected in parallel at the electrical bus. The sum of the currents into the DC bus from the six buoys can be calculated as

$$i_{ptosum} = \sum_{i=1}^{N} i_{pto,i}. \tag{6}$$

The DC electrical bus is modelled as a parallel combination of a resistor, capacitor, and ideal ESS. The substation is connected to the onshore electrical grid by a 1 km long undersea cable. The onshore electrical grid connection is modelled by a capacitor and resistor in parallel with a current source to represent the power injected to the grid by the WEC array. The substation can be modelled as

$$\dot{v_b} = \frac{1}{C_b}(i_{ptosum} - \frac{v_b}{R_b} - u - i_L) \tag{7}$$

where u is the ideal current injected into the substation from the ESS as

$$u = \frac{v_{sc} - v_b}{R_{ESR}}. \tag{8}$$

The undersea cable and grid connection can be modelled as

$$\dot{i_L} = \frac{1}{L_L}(v_b - i_L R_L - v_g) \tag{9}$$

$$\dot{v_g} = \frac{1}{C_g}(i_L - i_{grid} - \frac{v_g}{R_g}). \tag{10}$$

The variables used for the electrical and mechanical systems of the array can be found in Table I.

TABLE I
SYSTEM PARAMETER DESCRIPTIONS

Parameter	Description	Units
m	Buoy Mass	kg
c	Buoy Damper Coefficient	$N/\frac{m}{s}$
k	Buoy Spring Coefficient	$\frac{N}{m}$
f_e	Wave Excitation Force	N
r	Rack and Pinion Gear Radius	m
v_a	PMDC Armature Voltage	V
i_a	PMDC Armature Current	A
K_m	PMDC Torque Constant	$\frac{Nm}{A}$
L_a	PMDC Armature Inductance	H
R_a	PMDC Armature Resistance	Ω
v_b	PTO Collection Bus Voltage	V
i_l	Line Current	A
v_g	Grid side Voltage	V
v_{sc}	ESS Voltage	V
i_{pto}	Current from Electric Machine Drive	A
i_{grid}	Current into Grid Inverter	A
u	Current from ESS	A
C_b	Bus Capacitance	F
R_b	Bus Parasitic Resistance	Ω
C_g	Grid Inverter Resistance	A
R_g	Grid Inverter Resistance	Ω
R_{ESR}	Equivalent Series Resistance of C_b	Ω

C. Controls

The motion of the waves that the WEC array is located in exerts a force on each of the buoys. The excitation force on the WEC array was modelled in Equation 2. Any given sea state that the WEC array will be operating in can be described as the sum of of each of the individual frequency components that are summed together to create the irregular wave as

$$f_e = \sum_{n=1}^{N} A_n sin(w_n t + \phi_n). \tag{11}$$

This excitation force can be decomposed into its individual frequency components as

$$\hat{f_e}(t) = a_0 + \sum_{n=1}^{N} [a_n cos(n\omega t) + b_n sin(n\omega t)] \tag{12}$$

where a_0 is the average value of $f_e(t)$, and the amplitudes of the sine and cosine components of one frequency in the wave force summation are a_n and b_n respectively.

To extract the maximum energy from the wave force each WEC must resonate with the peak frequencies in the wave spectrum. To resonate with the peak frequencies of the wave the amplitudes of the individual frequency components must be calculated and a controller must be designed for each of the peak frequencies. Using a Sequential Least Squares Estimator (SLSE) the amplitudes of the sine and cosine components of each individual frequency can be calculated as

$$x_n = [a_1, b_1, ..., a_n, b_n]^T = x_{n-1} + PA^T(Y - Ax_{n-1}) \tag{13}$$

where the weighting matrix is P, A is the matrix containing the amplitudes for the sine and cosine components of the frequency, Y is the measured values to be estimated, and x_{n-1} is the previous sine and cosine amplitude estimates for an individual frequency [16].

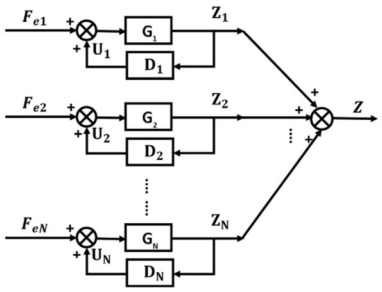

Fig. 2. Block diagram of the decomposed excitation force and PDC3 [7].

The calculated amplitudes for the frequency components can be used to implement PDC3 on the WEC array [7], [8], [1]. PDC3 requires that the multi-frequency excitation force acting on the WEC array be broken down into its individual frequency components. A PD controller can then be designed for each individual frequency to implement C3. The individual frequency control channels will then be summed together to create the full control force acting on the buoy. This process is shown in 2

The proportional gain in PDC3 is calculated to resonate the WEC with an individual frequency component of the full wave spectrum. The proportional gain is calculated as

$$k_{p,i} = \omega_i^2 m_i - k_i. \tag{14}$$

The derivative gain in the PD controller is designed to maximize the power absorbed by the buoy by setting the real portion of the control impedance equal to the real part of the mechanical impedance. The derivative gain is calculated as

$$k_{d,i} = c_i. \tag{15}$$

The sum of the individual frequency control channels is then used to provide the complete control force for each of the WECs operating in an irregular wave climate. The wave height and the frequencies of the sea-state that the WEC array is operating in can be compiled and described with a Bretschneider spectrum. Using the `Bretschneider` function in Wave Analysis for Fatigue Oceanography (WAFO) toolbox for MATLAB a Bretschneider spectrum can be created by entering the significant wave height and the peak frequency of a desired sea state [17]. The values for the significant wave height and peak frequency were collected from the National Data Buoy Center, buoy number 46073, and are shown in **Table** [18]. The frequency spectrum generated by the `Bretschneider` function was converted to the time domain using the WAFO `spec2dat` function. The mean water level that was generated with the `spec2dat` function was then scaled to represent a wave force acting upon the WEC array.

The PDC3 controller on each of the WECs puts the buoy into resonance with the incoming wave, and creates a power factor of one. In regular waves each WEC will output power as

$$p_i(t) = cos^2(\omega_n t) = \frac{1}{2}(cos(2\omega_n t) + 1). \tag{16}$$

.

In a WEC array each buoy is shifted in the water which will cause a phase shift, ϕ, in the electrical signals from the WECs. When the electrical signals from each WEC in the array are shifted at phase ϕ and the wave is at a frequency of ω_n, the power output from each WEC becomes

$$p_i(t) = \frac{1}{2}(cos(2\omega_n t - 2(i-1)\phi) + 1). \tag{17}$$

The sum of all the powers of N WECs in an array is

$$P_{array} = \sum_{i=1}^{N} p_i(t) \tag{18}$$

$$= \frac{1}{2}(csc(\phi)sin(N\phi)cos(2\omega_n t + \phi(1-N))) + N). \tag{19}$$

The sum of the total powers will be constant when

$$csc(\phi)sin(N\phi) = 0. \tag{20}$$

This happens at a phase shift of

$$\phi \in \left\{ \frac{\pi}{N}, \frac{2\pi}{N} \right\}. \tag{21}$$

Therefore if the six WECs of the array are positioned and paired to behave as three, they will produce a constant total output power when the WECs are position in the water as to produce a "phasing" of $\pi/3\ rad = 60^o$ or $2\pi/3\ rad = 120^o$ apart in time [19].

Having a constant output power from the WEC array has many advantages including: the reduced need for energy storage, a reduction in the ripple of the voltage in the electrical collection bus, and a decrease in power losses which leads to an increase in power delivered to the electrical grid. Since the WEC array is operating in an irregular wave climate, which is composed of multiple frequencies, there may not be phase or time shift that results in constant power but instead a phase shift that results in minimal power variation.

D. Cost Function

In addition to phase shifting the buoys the placement of the buoys in the water can be angled with respect to the incoming wave force and the rate at which the current injected into the grid is updated can be changed to minimize the power variation of the WEC array. Using MATLAB's built in nonlinear optimizer `fmincon` the time shift between buoys, degree shift, and grid update rate are utilized to minimize the power variation cost function. `Fmincon` takes a nonlinear cost function and the initial values of the variables that will be manipulated in the Simulink model to minimize the given cost function. The initial values input into the `fmincon` function are shown in Table VI.

The cost function to minimize the power variation for the WEC array is designed to minimize the variation in the bus voltage, and minimize the energy and power of the ESS while maximizing the energy delivered to the grid. The input variables into the cost function include the time shift between buoys, the degree shift of the incident wave, and the grid update rate. The cost function input into MATLAB's `fmincon` function

$$J = x_{GE}/GE + ESS_E/x_{ESSE} + \Delta V_b/x_{V_b} + ESS_P/x_{ESSP} \tag{22}$$

where the weighting factors x_{GE}, x_{ESSE}, x_{V_b}, and x_{ESSP} were initially set to a value of one and then updated with the minimized or maximized values of their respective variables to equalize the importance of each of the variables on the overall cost.

TABLE II
VARIABLES TO MINIMIZE OR MAXIMIZE IN THE COST FUNCTION.

Parameter	Variable	Minimize of Maximize
Variation in Bus Voltage	ΔV_b	Minimize
ESS Energy	ESS_E	Minimize
ESS power	ESS_P	Minimize
Grid Energy	GE	Maximize

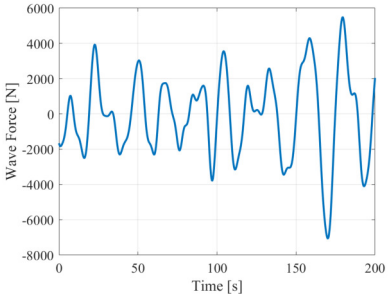

Fig. 3. The excitation force of the Bretschneider wave $\hat{f}_e(t)$.

TABLE III
FREQUENCY CHANNELS USED IN PDC3 CONTROLLER

Channel	Frequency (Hz)
1	0.0435
2	0.0575
3	0.0460
4	0.0360

III. SIMULATION RESULTS

The excitation force in the MATLAB/Simulink model was developed from the Bretschneider Spectrum. The toolbox that was used to create the wave force is outlined in Section II-C. The generated wave force is shown in Figure 3 The wave force was then transformed into the frequency domain using MATLAB's built in Fast Fourier Transform (FFT) function. The frequency domain of the excitation force was used to determine the peak frequencies of the excitation force. The four peak frequencies from the wave force frequency spectrum were chosen to tune the four PDC3 controller channels on each of the WECs. The peak frequencies used to tune the PDC3 channels are shown in III. These four frequency channels are used in the SLSE as described in Section II-C to estimate the amplitudes of each of these frequency components in the total Bretschneider excitation force.

TABLE IV
RESULTS VARYING TIME SHIFTS ON THE 6 WECS

Δt [s]	Degree Shift [^{o}]	Pk-Pk Voltage Noise [%]	ESS Energy [kJ]	Grid Power [kW]
0		3.19	157.07	2.36
1		3.61	92.80	2.12
2		2.52	240.53	2.68
3	∼60	0.79	69.11	4.09
4	∼60	1.22	69.13	4.28
5		1.44	135.20	4.06
6		0.80	422.32	2.29
7	∼120	2.00	396.05	2.32

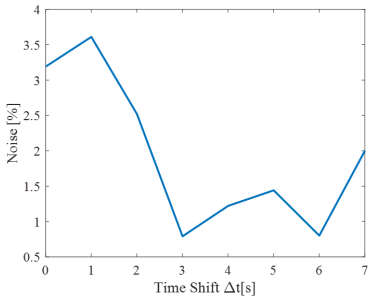

Fig. 4. Percent Noise of the Nominal Bus Voltage for Changing Δt

The six WEC array was first simulated by changing the time shift between the buoys in 1 second increments. These simulations show that changing the Δt variable has dramatic effects on the noise in the bus voltage, the energy stored in the ESS, and the power exported to the grid. The variations in the bus noise, ESS energy, and grid power for changing Δt between the buoys are shown in Figures 4, 5, and 6.

From these results it can be determined that time shifting the buoys with respect to each other will minimize the ESS size and bus voltage noise while maximizing the power delivered to the grid. As discussed in Section II-C the optimal time shifting will be observed around 60^o or 120^o. The peak frequency in the Bretschneider wave force is 0.0435 Hz. The peak period is 22.98 seconds, so a phase shift of 120^o is 7.66 seconds and a phase shift of 60^o is 3.83 seconds between buoys. Table IV shows the time shifting in seconds compared to the phase shift between the signals and the effect on the bus voltage noise, ESS size, and exported grid power.

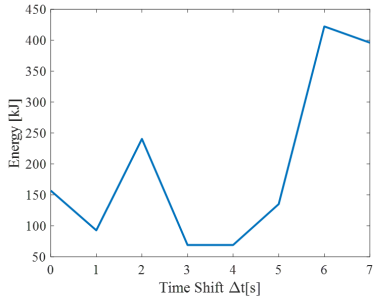

Fig. 5. Total Energy Stored in the ESS for Changing Δt

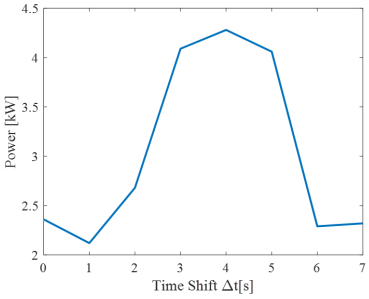

Fig. 6. Total Power Exported to the Grid for Changing Δt

TABLE V
RESULTS VARYING THE ANGLE OF THE WAVE FORCE

Degree [^{o}]	Pk-Pk Voltage Noise [%]	ESS Energy [kJ]	Grid Power [kW]
0	1.23	69.13	4.28
5	1.23	68.07	4.16
10	1.32	68.97	4.29
15	1.49	74.22	4.01
20	1.69	81.32	4.07
25	1.80	81.88	4.167
30	1.84	81.89	3.85
35	1.95	76.59	4.09
40	1.85	77.78	4.185
45	1.59	149.37	3.77

TABLE VI
INITIAL VALUES FOR FMINCON COST FUNCTION INPUT VARIABLES.

Variable	Value
Δt	4 [s]
Degree Shift	10^o
Grid Update Rate	4 [s]

The optimal time shift between buoys was determined to be 4 seconds as this produced the most advantageous combination between minimizing the bus voltage noise and ESS size while maximising the power output to the grid for the array. The six WEC array was then simulated with a four second time shift between the buoys and angling the incident wave in increments of 5^o. The results for angling the incident wave are shown in Table V. The results in Table V show that the WEC array exports more power to the grid when the angle of the wave is relatively small. The results in Table IV show that the WEC array exports the most power to the grid at four seconds. When running the `fmincon` optimizer it is expected that the optimal time shift will be around 4 seconds and the optimal angle will be relatively small.

The final simulations ran on the Simulink/MATLAB WEC array included using the `fmincon` cost function developed in Section II-D. The initial values for the input variables used in the cost function are shown in Table VI.

The model was then run using the nonlinear optimizer to determine the optimal values for the time shift between buoys, the degree shift of the incident wave, and the grid update rate to minimize bus voltage noise, ESS power and ESS energy while maximizing the energy exported to the grid. The optimal

TABLE VII
OPTIMIZED VALUES FOR FMINCON COST FUNCTION INPUT VARIABLES.

Variable	Value
Δt	3.91 [s]
Degree Shift	1.20^o
Grid Update Rate	2.46 [s]

TABLE VIII
VARIABLES TO MINIMIZE OR MAXIMIZE IN THE COST FUNCTION.

Parameter	Variable	Value
Variation in Bus Voltage	ΔV_b	0.72%
ESS Energy	ESS_E	60.8 kJ
ESS power	ESS_P	9.48 kW
Grid Energy	GE	462.3 kJ
Avg. Grid Power	GP	3.92 kW

values for the time shift between buoys, the degree shift of the wave, and the grid update rate determined using the `fmincon` function are shown in Table VII. The minimized values for the ESS energy, ESS power, and the variation in the bus voltage as well as the maximized value for the energy exported to the grid and the average grid power are shown in Table VIII.

The results show that around a 60^o phase shift between the electrical signals, which corresponds to a time shift of $3.8\ s$, the power variation in the WEC array will be minimized while the power exported to the grid will be maximized. In addition to a time shift between the buoys, angling the six WEC array with respect to the incident wave will further minimize the power variation across the electrical components and maximize the power delivered to the grid.

IV. CONCLUSION

This paper implements PDC3 on an array of 6 WECs and shows that the spacing of WECs in an irregular wave climate dramatically effects the necessary energy storage of the WEC array and power delivered to the grid. The WECs were configured in a hexagonal array and the spacing between the pairs of WECs was explored to determine the optimal shift that would cause the most advantageous phase shift in the electrical signals from each buoy. The optimal shift of the WEC array was then explored further by angling the wave force interacting with the WECs to further decrease the energy storage requirements and maximize the delivered grid power. The WEC array was further optimized by developing a cost function to minimize the power variation and the ESS size while maximizing the energy delivered to the grid.

V. ACKNOWLEDGMENT

This study was funded by the Laboratory Directed Research & Development (LDRD) program at Sandia National Laboratories. Sandia National Laboratories is a multi-mission laboratory managed and operated by National Technology and Engineering Solutions of Sandia, LLC., a wholly owned subsidiary of Honeywell International, Inc., for the U.S. Department of Energy's National Nuclear Security Administration under contract DE-NA0003525. This paper describes objective technical results and analysis. Any subjective views or opinions that might be expressed in the paper do not necessarily represent the views of the U.S. Department of Energy or the United States Government. Special thanks to Dr. Ray Byrne at Sandia, for his technical review and programmatic leadership for this LDRD project.

REFERENCES

[1] J. Song, O. Abdelkhalik, R. Robinett, G. Bacelli, D. Wilson, and U. Korde, "Multi-resonant feedback control of heave wave energy converters," *Ocean Engineering*, vol. 127, pp. 269–278, 2016.

[2] P. T. Jacobson, G. Hagerman, and G. Scott, "Mapping and assessment of the united states ocean wave energy resource," Electric Power Research Institute, Tech. Rep., 2011.

[3] M. Chen and H. V. Poor, "High-frequency power electronics at the grid edge: A bottom-up approach toward the smart grid," *IEEE Electrification Magazine*, vol. 8, no. 3, pp. 6–17, 2020.

[4] W. W. Weaver, D. G. Wilson, A. Hagmuller, M. Ginsburg, G. Bacelli, R. D. Robinett, R. Coe, and B. Gunawan, "Super capacitor energy storage system design for wave energy converter demonstration," in *IEEE International Symposium on Power Electronics, Electrical Drives, Automation and Motion*, 2020, pp. 564–570.

[5] D. G. Wilson, W. W. Weaver, G. Bacelli, and R. D. Robinett, "Wec array electro-mechanical drivetrain networked microgrid control design and energy storage system analysis," in *2018 International Symposium on Power Electronics, Electrical Drives, Automation and Motion (SPEEDAM)*. IEEE, 2018, pp. 1278–1285.

[6] J. Prendergast, M. Li, and W. Sheng, "A study on the effects of wave spectra on wave energy conversions," *IEEE Journal of Oceanic Engineering*, vol. 45, no. 1, pp. 271–283, 2018.

[7] D. G. Wilson, G. Bacelli, R. D. Robinett, U. A. Korde, O. Abdelkhalik, and S. F. Glover, "Order of magnitude power increase from multi-resonance wave energy converters," in *OCEANS 2017-Anchorage*. IEEE, 2017, pp. 1–7.

[8] O. Abdelkhalik, S. Zou, R. D. Robinett, G. Bacelli, D. G. Wilson, R. Coe, and U. Korde, "Multiresonant feedback control of a three-degree-of-freedom wave energy converter," *IEEE Transactions on Sustainable Energy*, vol. 8, no. 4, pp. 1518–1527, 2017.

[9] F. Fusco and J. V. Ringwood, "A simple and effective real-time controller for wave energy converters," *IEEE Transactions on sustainable energy*, vol. 4, no. 1, pp. 21–30, 2012.

[10] J. Falnes and A. Kurniawan, *Ocean waves and oscillating systems: linear interactions including wave-energy extraction*. Cambridge university press, 2020, vol. 8.

[11] G. Bacelli, *Optimal control of wave energy converters*. National University of Ireland, Maynooth (Ireland), 2014.

[12] M. G. Veurink, W. W. Weaver, R. D. Robinett, D. G. Wilson, and R. C. Matthews, "Wave energy converter optimization with multi-resonance controller of the electrical power take-off," in *2022 IEEE Power and Energy Conference at Illinois (PECI)*. IEEE, 2022, pp. 1–5.

[13] D. G. Wilson, R. D. Robinett III, G. Bacelli, O. Abdelkhalik, and R. G. Coe, "Extending complex conjugate control to nonlinear wave energy converters," *Journal of Marine Science and Engineering*, vol. 8, no. 2, p. 84, 2020.

[14] D. G. Wilson, R. D. Robinett, W. W. Weaver, M. G. Veurink, and S. F. Glover, "Wec arrays with power packet networks for efficient energy storage and grid integration," in *OCEANS 2021: San Diego–Porto*. IEEE, 2021, pp. 1–8.

[15] J. Toyoda and H. Saitoh, "Proposal of an open-electric-energy-network (oeen) to realize cooperative operations of iou and ipp," in *Proceedings of EMPD '98. 1998 International Conference on Energy Management and Power Delivery (Cat. No.98EX137)*, vol. 1, 1998, pp. 218–222 vol.1.

[16] J. L. Crassidis and J. L. Junkins, *Optimal estimation of dynamic systems*. Chapman and Hall/CRC, 2004.

[17] T. Perez and T. I. Fossen, "A MATLAB toolbox for parametric identification of radiation-force models of ships and offshore structures," 2009.

[18] "Southeast bering sea - 205 NM WNW of Dutch Harbor, AK," https://www.ndbc.noaa.gov/station_page.php?station=46073, Accessed: 2021-11-06.

[19] S. Husain, G. G. Parker, and W. W. Weaver, "Storage minimization of marine energy grids using polyphase power," *Journal of Marine Science and Engineering*, vol. 10, no. 2, p. 219, 2022.